INSTITUTE OF PHYSICS PUBLISHING JOURNAL OF PHYSICS: CONDENSED MATTER

J. Phys.: Condens. Matter **17** (2005) S67–S75 doi:10.1088/0953-8984/17/5/008

Refinement of the Si–O–Si bond angle distribution in vitreous silica

M G Tucker[1], D A Keen[2,3], M T Dove[1] and K Trachenko[1]

[1] Department of Earth Sciences, Cambridge University, Downing Street, Cambridge CB2 3EQ, UK
[2] Physics Department, Oxford University, Clarendon Laboratory, Parks Road, Oxford OX1 3PU, UK
[3] ISIS Facility, Rutherford Appleton Laboratory, Chilton, Didcot, Oxon OX11 0QX, UK

E-mail: d.a.keen@rl.ac.uk

Received 30 November 2004
Published 21 January 2005
Online at stacks.iop.org/JPhysCM/17/S67

Abstract

A model of silica glass consisting of a fully connected corner-sharing network of SiO_4 tetrahedra is refined using neutron diffraction data and reverse Monte Carlo modelling. This model is then used to investigate optimal inter-tetrahedral Si–O–Si bond angle distributions. The distribution which is most consistent with the data is found to be centred around $\theta_{Si-O-Si} = 151.0°$ with a standard deviation of between 9° and 12°. Other recent determinations of the Si–O–Si bond angle distribution are in good agreement with this result.

(Some figures in this article are in colour only in the electronic version)

1. Introduction

Amorphous silica is considered the archetypal network glass. As such its structure has been extensively studied using a variety of techniques including neutron diffraction [1], x-ray diffraction [2, 3], nuclear magnetic resonance (NMR) spectroscopy [4, 5] and Monte Carlo (MC) [6] and molecular dynamics (MD) [7] simulations. The general consensus of these studies is that the structure consists of a continuous random network of fully connected corner-sharing SiO_4 tetrahedral units. However, within this descriptive framework, considerable variety in the longer-range structure may be envisaged. One example of this is the much-discussed distribution of Si–O–Si inter-tetrahedral bond angles. This bond angle distribution is fundamental in so far as it determines the nature of the longer-range network topology and hence many of the physical properties of silica glass. It should also provide a clear indicator of the relative efficacy of simulated glass structures. The uncertainty in seemingly trivial structural parameters arises from the difficulty in interpreting available experimental structural information from a disordered system in a direct and unambiguous manner and without recourse to theoretical assumptions [8].

A large number of Si–O–Si bond angle distributions have been proposed. An early x-ray diffraction measurement was interpreted using a mean Si–O–Si bond angle, $\langle\theta_{\mathrm{Si-O-Si}}\rangle$, of $\sim$144° and a full width half maximum (FWHM) of $\sim$35° [2]. More recent high energy synchrotron x-ray diffraction measurements [3], combined with neutron diffraction [1], have been analysed using a local model to yield $\langle\theta_{\mathrm{Si-O-Si}}\rangle = 147°$ and an FWHM of 17° [9]. This is a significantly narrower distribution than that proposed using a different model based on the x-ray data alone [3], and its width has recently been challenged [10]. There have also been a large number of NMR measurements on silica, of increasing complexity, aimed at determining this Si–O–Si bond angle distribution. Si–O–Si bond angle distributions from NMR tend to be sharper than those from diffraction; for example, interpretation of ^{29}Si MAS NMR gave an asymmetric distribution with $\langle\theta_{\mathrm{Si-O-Si}}\rangle = 143°$ and an FWHM of $\sim$20° [11]; similar distributions have been obtained using ^{17}O dynamic angle spinning NMR [12] although very recent DAS measurements suggest $\langle\theta_{\mathrm{Si-O-Si}}\rangle = 147°$ with a standard deviation, $\sigma_{\mathrm{Si-O-Si}} = 3.8°$ [13].

Recent MC models [6] using different Keating type potentials [14] have $\langle\theta_{\mathrm{Si-O-Si}}\rangle$ ranging between 133° and 148° with $\sigma_{\mathrm{Si-O-Si}}$ between 12° and 14°. Similarly, classical MD studies produced a wide variety of $\langle\theta_{\mathrm{Si-O-Si}}\rangle$ between 140° and 160° (see [15, 16] for summaries of early work and [7]). Several of these studies incorporated terms in their potentials which favoured particular Si–O–Si bond angles (for example [16], where the $\langle\theta_{\mathrm{Si-O-Si}}\rangle$ in the final model mimicked the mean position of the three-body Si–O–Si term in the potential). Even very recent classical MD simulations of silica using two-body and three-body potentials have produced very different Si–O–Si bond angle distributions [10]. *Ab initio* MD simulations tend to yield lower $\langle\theta_{\mathrm{Si-O-Si}}\rangle$ (e.g. $\langle\theta_{\mathrm{Si-O-Si}}\rangle = 136° \pm 14°$ [8]). More recent 'combined' classical and *ab initio* MD simulations give values of $145° \pm 13°$ [17]. The same group also used classical MD to investigate the effect of long-range forces on the Si–O–Si bond angle distribution; values for $\langle\theta_{\mathrm{Si-O-Si}}\rangle$ nearer 150° were obtained as the strength of the Coulomb interaction increased [18].

Reverse Monte Carlo (RMC) modelling [19] has proved effective in the determination of disordered structures using neutron and/or x-ray diffraction data [20]. This method has been applied to amorphous silica in the past to good effect [21, 22]. The method consists of moving atoms chosen randomly a random amount within a three-dimensional configuration of atoms under periodic boundary conditions. Each time an atom is moved the difference between structural functions calculated from the configuration and those measured experimentally (such as the total scattering structure factor, $S(Q)$) is determined. If the agreement improves, then the move is accepted, and if the agreement worsens, then the move is accepted with a reduced probability. It was found that the modelling method by itself is most likely to yield a structure with a partially connected network (for example, one such RMC generated model had, on average, 3.7 oxygen atoms surrounding each Si atom [21]). The effect of this is to introduce deficiencies in other aspects of the structure to counteract the reduced coordination. Examples of this might be a small proportion of unphysically distorted SiO_4 tetrahedra or structures with a larger number of rings of smaller size than normally expected. (Here 'rings' refer to the shortest number of silicon atoms, joined via bridging oxygen atoms, that are passed through within the structure in order to return to the starting silicon atom.)

The RMC method was therefore adapted to refine a model with a predetermined chemically correct network topology maintained by nearest neighbour bonding constraints. RMC *refinement*, although departing somewhat from the original philosophy of RMC *modelling*, has been used to good effect recently on crystalline framework structures to characterize their disordered structures and to investigate local changes during phase transitions and similarities in local disordered structures within distinct crystalline phases [23]. An initial structure of

Table 1. Ring statistics of the two fully connected models of silica glass used in this work (expressed as percentages).

Ring size	4	5	6	7	8	9	10
MD1	0.0	18.1	42.2	27.0	10.3	2.3	0.2
MD2	0.3	17.6	39.7	31.3	8.8	2.2	0.2

vitreous silica, constructed using a simple model building algorithm, was also refined using RMC modelling [22]. The connectivity was better (on average, 3.9 oxygen atoms were coordinated to each Si atom), the SiO_4 tetrahedra were less distorted and the fit to the data was improved. However, the structure was still not fully connected and now that fully connected models are available of suitable size (see below), the structure of silica has been reexamined using RMC refinement. The results are detailed in this paper.

The method for producing starting models of fully connected tetrahedral networks of silica glass has been described previously [24] and involves randomizing and relaxing the diamond structure to produce a model of amorphous silicon with periodic boundary conditions [25]. Two such models each of 512 Si atoms were kindly provided by Professor M F Thorpe. The proportions of different sized rings for these two models are listed in table 1. This shows that the topology of both models is very similar, with neither model possessing three-fold rings, although MD2 has a very small number of four-fold rings. Oxygen atoms were then inserted mid-way between each pair of silicon atoms and the SiO_2 structural models were further relaxed using an MD simulation to produce (for example) more physically realistic nonlinear Si–O–Si linkages [24].

2. Experiment and RMC refinement

Neutron diffraction data from a 10 mm diameter rod of pure silica glass were collected on the GEM total scattering diffractometer at ISIS [26]. The data were corrected in the usual manner [27] to produce a total scattering structure factor, $S(Q)$ [28]. The silica models were refined using RMC and by minimizing the following function:

$$\chi^2_{\mathrm{RMC}} = \chi^2_{\mathrm{Data}} + \chi^2_{\mathrm{Constraints}} \tag{1}$$

where

$$\chi^2_{\mathrm{Data}} = \sum_k \sum_{i=1}^{n} [S_{\mathrm{calc}}(Q_i) - S_{\mathrm{exp}}(Q_i)]^2/\sigma(Q_i) + \sum_{i=1}^{m} [T_{\mathrm{calc}}(r_i) - T_{\mathrm{exp}}(r_i)]^2/\sigma(r_i) \tag{2}$$

and

$$\chi^2_{\mathrm{Constraints}} = w_{\mathrm{Si-O}} \sum_{\mathrm{Si-O}} (r_{\mathrm{Si-O}} - R_{\mathrm{Si-O}})^2 + w_{\mathrm{O-Si-O}} \sum_{\mathrm{intra}} (\theta_{\mathrm{O-Si-O}} - \Theta_{\mathrm{O-Si-O}})^2 + w_{\mathrm{Si-O-Si}} \sum_{\mathrm{inter}} (\theta_{\mathrm{Si-O-Si}} - \Theta_{\mathrm{Si-O-Si}})^2 \tag{3}$$

summing over the n data points in $S(Q)$ from each of the k detector banks, the m data points in $T(r)$, all the Si–O bonds and all the intra- and inter-tetrahedra bond angles in the model, respectively. $R_{\mathrm{Si-O}}$ and $\Theta_{\mathrm{O-Si-O}}$ are the mean intra-tetrahedral Si–O distance (obtained from the lowest peak in the real space total pair distribution function, $T(r)$) and angle (109.47°), respectively. $\Theta_{\mathrm{Si-O-Si}}$ is the required mean inter-tetrahedral angle. The σ and w parameters determine the relative weighting of the separate terms in equation (1) and, with the exception of $w_{\mathrm{Si-O-Si}}$, were kept fixed throughout. Both $w_{\mathrm{Si-O}}$ and $w_{\mathrm{O-Si-O}}$ were chosen to maintain

Table 2. Summary of the various models of silica used in this study with unconstrained Si–O–Si bond angle distributions. (22) refers to a previous model [22]; MD2 (MD1) does (does not) contain four-membered rings; the linear model refers to an initial model with linear Si–O–Si bonds of the same topology as MD1. The fourth and fifth columns list the mean and standard deviation of the Si–O–Si bond angle distributions, respectively.

Model	No of tetrahedra	χ^2_{Data}	$\langle\theta_{\mathrm{Si-O-Si}}\rangle$ (deg)	$\sigma(\theta_{\mathrm{Si-O-Si}})$ (deg)
(22)	1000		n/a	
RMC of (22)	1000	120	139	20
MD1	512	950	148.8	12.7
RMC of MD1	512	44	152.6	12.0
MD2	512	980	149	12.6
RMC of MD2	512	60	152.7	11.8
Linear	512	1188	180	0
RMC of linear	512	54	150	12.8

the integrity of the tetrahedra and network connectivity, and to reproduce the low-r Si–O and O–O peaks in $T(r)$.

3. Results

Table 2 compares the mean and standard deviation of the Si–O–Si bond angle distribution of a number of different silica models before and after refinement using RMC modelling (with $w_{\mathrm{Si-O-Si}} = 0$). None of the initial models agree particularly well with the data. The MD models tend to have too sharp intra-tetrahedral correlations, leading to large amplitudes in the high-Q features of $S(Q)$. However, all the models give a good agreement to the data after RMC refinement. The least good is the earlier RMC model [22], and this is attributed to the effect of non-bridging oxygen atoms and the presence of three-membered rings in the model. The next least good is model MD2 ($\chi^2_{\mathrm{Data}} = 60$). It is not entirely clear why this model should be worse than model MD1 ($\chi^2_{\mathrm{Data}} = 44$), although most likely it is a consequence of the different ring statistics of the two models. There are, for example, a small number of four-membered rings in MD2. It is also interesting that the agreement is different for the two models which originated from the same amorphous silicon configuration. The χ^2_{Data} for the 'linear' model which only used RMC refinement without an intermediate MD step was slightly worse ($\chi^2_{\mathrm{Data}} = 54$ compared with $\chi^2_{\mathrm{Data}} = 44$ for MD1). This shows that, although both have the same topology, the intermediate bond relaxation stage used in MD1 (moving all atoms simultaneously during each time step) allowed the model to achieve a lower global minimum than the linear model, where the relaxation was effected entirely by the data during RMC refinement (moving atoms one at a time). Significant large-scale, low-energy rearrangements of the silica structure have previously been observed during MD simulations [24].

The quality of the fit to the data for the RMC refined model MD1 is shown in figure 1, with the partial radial distribution functions from the same model in figure 2. The agreement with the experimental $T(r)$ and $S(Q)$ is very good, although the model does not capture the full height of the first diffraction peak in $S(Q)$. The partial radial distribution functions all look very sensible, with good separation, even $g_{\mathrm{Si-Si}}(r)$ (which has a low neutron weight in $S(Q)$). The separation could perhaps have been improved by including x-ray $S(Q)$ data in the RMC modelling, but this was not done for reasons of computational speed and a concern that the neutron and x-ray datasets may not have been fully consistent. For completeness, the bond angle distributions are shown in figure 3.

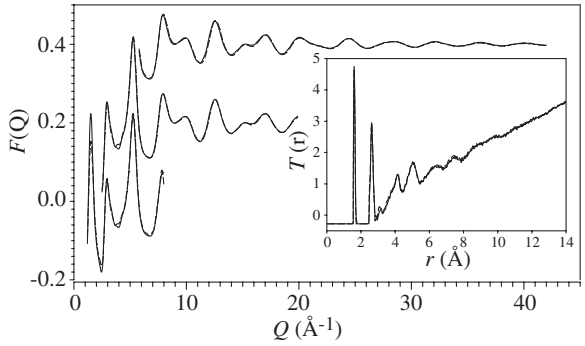

Figure 1. Plot showing the experimental neutron diffraction data. The structure factors from three different detector banks on GEM (main plot) and the pair distribution function (inset) (dashed curves) are compared with equivalent functions calculated from the RMC refined model MD1 (full curves).

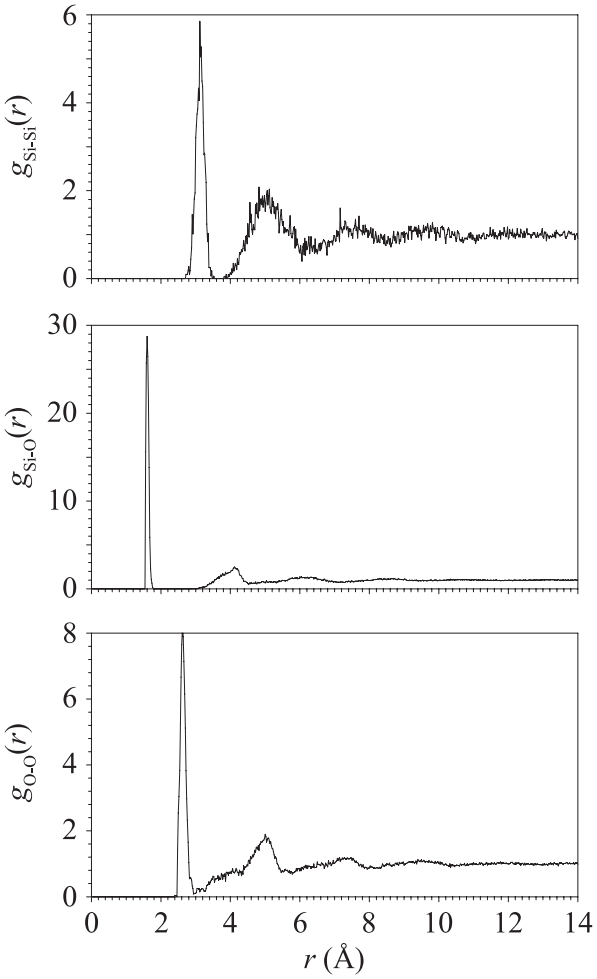

Figure 2. Partial radial distribution functions from the RMC refined model MD1.

In order to assess the impact of different Si–O–Si bond angle distributions on the fit to the data, a series of RMC refinements was carried out starting with the MD1 model for a range of $w_{\mathrm{Si-O-Si}}$ and $\Theta_{\mathrm{Si-O-Si}}$ but otherwise identical parameters. Each refinement was also run for the same length of time. The results are summarized in figures 4 and 5. Figure 4(a) shows that, even with the highest weighting on the Si–O–Si constraint, the mean value of the Si–O–Si

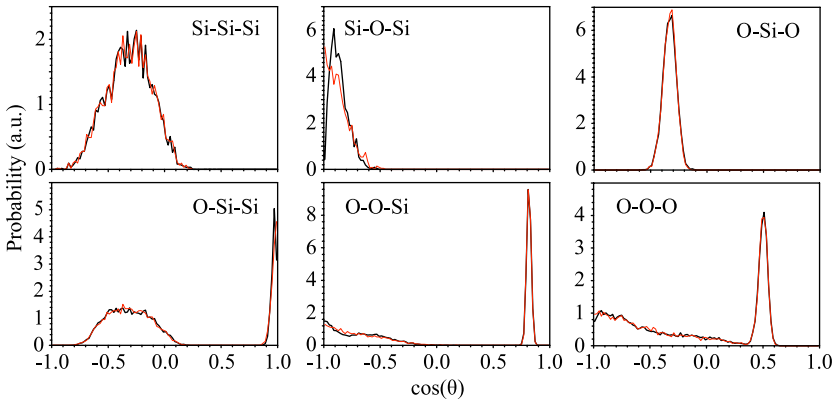

Figure 3. Bond angle distributions from RMC refinement of model MD1 (thin curve) and from RMC refinement of the same model with an optimized constraint on the inter-tetrahedral bond angle (thick curve). See the text for details.

distribution, $\langle\theta_{\mathrm{Si-O-Si}}\rangle$, from the RMC refined model only replicates the requested $\Theta_{\mathrm{Si-O-Si}}$ value around 150°. Figure 4(b) shows that the fit to the data becomes progressively worse as $\langle\theta_{\mathrm{Si-O-Si}}\rangle$ moves away from $\simeq$150°. Also, decreasing the $w_{\mathrm{Si-O-Si}}$ weighting produces a lower minimum in χ^2_{Data} until the lowest $w_{\mathrm{Si-O-Si}}$, when it increases very slightly. Closer inspection of this plot shows that the minimum in χ^2_{Data} occurs at slightly larger $\langle\theta_{\mathrm{Si-O-Si}}\rangle$ for lower values of $w_{\mathrm{Si-O-Si}}$. This is seen in figure 5, noting that smaller $w_{\mathrm{Si-O-Si}}$ gives rise to broader Si–O–Si bond angle distributions and hence larger $\sigma_{\mathrm{Si-O-Si}}$. The minimum around $\langle\theta_{\mathrm{Si-O-Si}}\rangle \simeq 150°$ becomes deeper as $\sigma_{\mathrm{Si-O-Si}}$ increases, before rising very slightly for $\sigma_{\mathrm{Si-O-Si}} > 10°$. The best agreement with the neutron diffraction data occurs in a region around $\langle\theta_{\mathrm{Si-O-Si}}\rangle \simeq 151°$ and $\sigma_{\mathrm{Si-O-Si}} \simeq 9°$ (typified by the minimum in the dot–dashed curve in figure 4(b)). It is also clear from figure 5 that, despite a wide range of $\Theta_{\mathrm{Si-O-Si}}$ (see figure 4(a)) and an almost two orders of magnitude change in $w_{\mathrm{Si-O-Si}}$, some combinations of $\langle\theta_{\mathrm{Si-O-Si}}\rangle$ and $\sigma_{\mathrm{Si-O-Si}}$ are inaccessible.

4. Discussion

The significance of the above result is two-fold. First, the optimum Si–O–Si bond angle distribution ($\langle\theta_{\mathrm{Si-O-Si}}\rangle = 151.0(5)°$ and $\sigma_{\mathrm{Si-O-Si}} = 9.0(5)°$) based on this systematic constrained study is not substantially different from that obtained from the RMC refinement with no Si–O–Si bond angle constraint ($\langle\theta_{\mathrm{Si-O-Si}}\rangle = 152.6(5)°$ and $\sigma_{\mathrm{Si-O-Si}} = 12.0(8)°$). The former has a slightly lower χ^2_{Data} and a narrower distribution, but the unconstrained RMC refinement is reasonable. This demonstrates that the RMC refinement method, if suitably applied, does not produce significantly inaccurate or overly disordered results. Secondly, and more importantly, the optimum Si–O–Si bond angle distribution should place a stringent test on other simulations of the silica glass structure. This is important given the wide variety of values obtained from simulations and the use of $\langle\theta_{\mathrm{Si-O-Si}}\rangle$ in some empirical potentials.

Although the centre of the distribution is different, this distribution (shown in figure 6) is similar to that of an earlier investigation using neutron and x-ray total scattering data [9] with a similar shape and width. Their model [9] was based on a chain of linked SiO_4 tetrahedra and was therefore not a fully connected three-dimensional structure with correct macroscopic density. Both neutron and x-ray total scattering data were used to refine the model, but the agreement with both these datasets was inferior to the RMC model presented here.

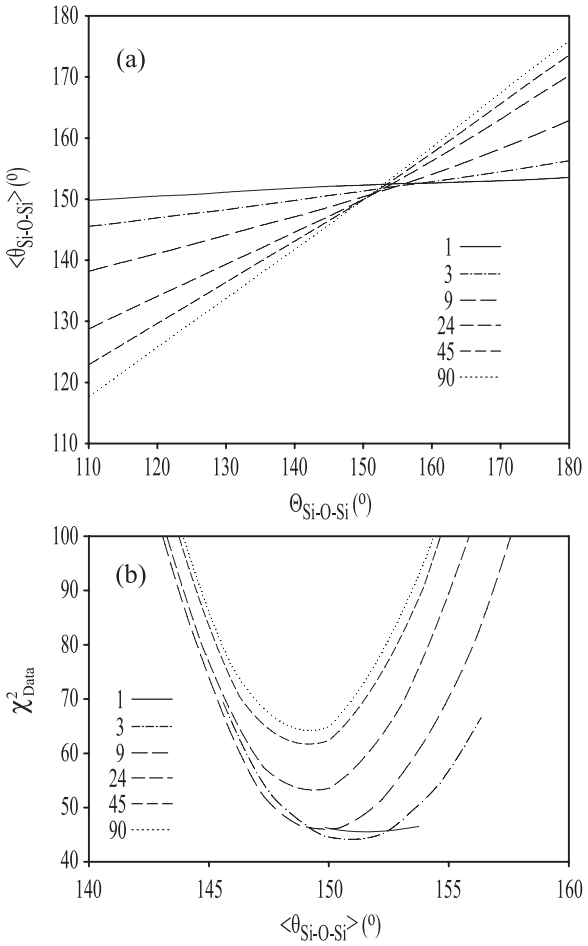

Figure 4. Plot showing (a) the mean value of the Si–O–Si bond angle distribution $\langle\theta_{\mathrm{Si-O-Si}}\rangle$ against the RMC refinement constraint $\Theta_{\mathrm{Si-O-Si}}$ and (b) variation of χ^2_{Data} with $\langle\theta_{\mathrm{Si-O-Si}}\rangle$, each for different values of $w_{\mathrm{Si-O-Si}}$ (shown as relative values in the legends).

However, since both investigations determine distributions of similar widths, the very narrow distributions sometimes found in ^{17}O NMR results [13] must be questioned. Instead, these results are consistent with another recent analysis of ^{29}Si NMR results [29]. In this instance the NMR signal is well described by either a symmetric Si–O–Si bond angle distribution function with $\langle\theta_{\mathrm{Si-O-Si}}\rangle = 150.6°$ and $\sigma_{\mathrm{Si-O-Si}} = 11.5°$ or by an asymmetric function with $\langle\theta_{\mathrm{Si-O-Si}}\rangle = 151.4°$ and $\sigma_{\mathrm{Si-O-Si}} = 11.3°$ (see figure 6).

The larger than often quoted value of $\langle\theta_{\mathrm{Si-O-Si}}\rangle$ could be challenged. However, this could be due to the network topology of this particular model which does not contain three-or four-membered rings; larger ring sizes are expected to have larger $\langle\theta_{\mathrm{Si-O-Si}}\rangle$. The effect of models with very different ring statistics (including significant numbers of three-and/or four-membered rings) has not been investigated in this study. It should also be noted that the uncertainties of some NMR fitting procedures are such that the values quoted for the RMC models here are within the error of the NMR values (for example [13] gives $\langle\theta_{\mathrm{Si-O-Si}}\rangle = 147°$ with an uncertainty of 4.4°).

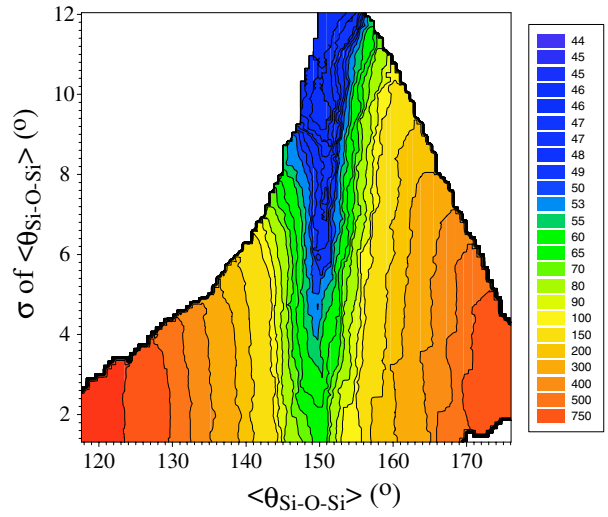

Figure 5. Contour plot showing the distribution of $\chi^2_{\rm Data}$ as a function of the mean value of the Si–O–Si bond angle distribution $\langle\theta_{\rm Si-O-Si}\rangle$ and its standard deviation $\sigma_{\rm Si-O-Si}$.

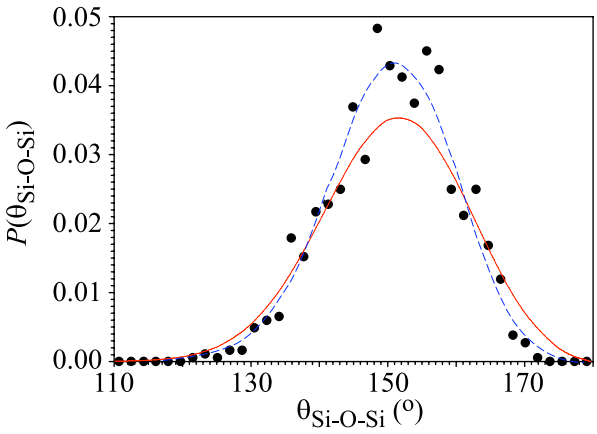

Figure 6. Distribution of the optimum Si–O–Si bond angle distribution in silica obtained by RMC refinement (points and dashed curve guide to the eye) with a recent symmetric function derived from NMR results (full curve) [29].

5. Conclusion

A definitive Si–O–Si bond angle distribution in silica glass has been obtained from a systematic series of RMC refinements of neutron diffraction data. The resultant distribution is consistent with recent distributions obtained from a recent analysis of NMR results [29]. The deficiencies in earlier RMC generated models may be attributed to the presence of non-bridging oxygen atoms in the structure. In the present study this has been overcome by starting with a configuration of fully connected corner-sharing SiO_4 tetrahedra, yielding a better fit to the data and a more robust final model.

References

[1] Grimley D I, Wright A C and Sinclair R N 1990 *J. Non-Cryst. Solids* **119** 49
[2] Mozzi R L and Warren B E 1969 *J. Appl. Crystallogr.* **2** 164
[3] Poulsen H F, Neuefeind J, Neumann H-B, Schneider J R and Zeidler M D 1995 *J. Non-Cryst. Solids* **188** 63
[4] Dupree E and Pettifer R F 1984 *Nature* **308** 523
[5] Mahler J and Sebald A 1995 *Solid State Nucl. Magn. Reson.* **5** 63
[6] von Alfthan S, Kuronen A and Kaski K 2003 *Phys. Rev.* B **68** 073203
[7] Rino J P, Ebbsjö I, Kalia R K, Nakano A and Vashishta P 1993 *Phys. Rev.* B **47** 3053
[8] Sarnthein J, Pasquarello A and Car R 1995 *Phys. Rev.* B **52** 12690
[9] Neuefeind J and Liss K-D 1996 *Ber. Bunsenges. Phys. Chem.* **100** 1341
[10] Yuan X and Cormack A N 2003 *J. Non-Cryst. Solids* **319** 31
[11] Gladden L F, Carpenter T A and Elliott S R 1986 *Phil. Mag.* B **53** L81
[12] Farnan I, Grandinetti P J, Baltisberger J H, Stebbins J F, Werner U, Eastman M A and Pines A 1992 *Nature* **358** 31
[13] Clark T M, Grandinetti P J, Florian P and Stebbins J F 2004 *Phys. Rev.* B **70** 064202
[14] Keating P 1966 *Phys. Rev.* **145** 637
[15] Kubicki J D and Lasaga A C 1988 *Am. Mineral.* **73** 941
[16] Vashishta P, Kalia R K, Rino J P and Ebbsjö I 1990 *Phys. Rev.* B **41** 12197
[17] Benoit M, Ispas S, Jund P and Jullien R 2000 *Eur. Phys. J.* B **13** 631
[18] Jund P, Rarivomanantsoa M and Jullien R 2000 *J. Phys.: Condens. Matter* **12** 8777
[19] McGreevy R L and Pusztai L 1988 *Mol. Simul.* **1** 359
[20] McGreevy R L 2002 *J. Phys.: Condens. Matter* **13** R877
[21] Keen D A and McGreevy R L 1990 *Nature* **344** 423
[22] Keen D A 1997 *Phase Transit.* **61** 109
[23] Dove M T, Tucker M G and Keen D A 2002 *Eur. J. Mineral.* **14** 331
[24] Trachenko K O, Dove M T, Harris M J and Heine V 2000 *J. Phys.: Condens. Matter* **12** 8041
[25] Wooten F and Weaire D 1987 *Solid State Physics* vol 40 (New York: Academic) p 1
[26] Williams W G, Ibberson R M, Day P and Enderby J E 1998 *Physica* B **241–243** 234
[27] Howe M A, McGreevy R L and Howells W S 1989 *J. Phys.: Condens. Matter* **1** 3433
[28] Keen D A 2001 *J. Appl. Crystallogr.* **34** 172
[29] Mauri F, Pasquarello A, Pfrommer B G, Yoon Y-G and Louie S G 2000 *Phys. Rev.* B **62** R4786